



Evaluation of anticancer, immunomodulatory and anti-inflammatory potential of antioxidant rich *Anzia ornatooides*, a lichen species from eastern Himalayan region



Pungbili Islary^a, Rajesh Kumar Meher^b, Suparna Biswas^a, Derhasat Basumatary^a,
Indra Bhusan Basumatary^c, Debasmita Dubey^d, Deepak Basumatary^e, Rebecca Daimari^{a,*}

^a Department of Botany, Bodoland University, Kokrajhar, Assam, India

^b Department of Biotechnology and Bioinformatics, Sambalpur University, Odisha, India

^c Department of Food Engineering and Technology, Central Institute of Technology, Assam, India

^d Medical Research Laboratory, IMS and SUM Hospital, Siksha 'O' Anusandhan Deemed to be University, Odisha, India

^e Department of English, Kokrajhar Government College, Kokrajhar, Assam, India

ARTICLE INFO

Article History:

Received 9 July 2023

Revised 8 November 2023

Accepted 24 November 2023

Available online 7 December 2023

Edited by: Dr. L. McGaw

Keywords:

Phytochemicals

Antioxidant

Anticancer

Apoptosis

Anzia ornatooides

Immunomodulatory

Toxicity

ABSTRACT

The lichen *Anzia ornatooides* was identified by its morpho-anatomical and chemical features. The hexane, diethyl ether, ethyl acetate, methanol, and water extracts of the lichen were assessed for their antioxidant capacities. The presence of various phyto-compounds of the methanol extract were run through a GC–MS and identified three major compounds viz. methoxyolivetol, imidazole 2-t-butyl-1,4-dimethyl-5-phenyl and benzoic acid 2,4-dihydroxy-3,6-dimethyl-methyl ester. The crude extraction of a lichen sample was carried out by Soxhlet apparatus. Total phenolic content was determined by Folin-Ciocalteu assay while flavonoid content was estimated using aluminium chloride assay. The antioxidant activity of the extracts was analysed by phosphomolybdenum assay, FRAP, DPPH, ABTS, and lipid peroxidation inhibition. To see the immunomodulatory and anti-inflammatory potential of the extracts, cell viability assay of macrophage was studied. In in-vitro anticancer activity, the extracts were explored using cancer cell line of different organ and tissue origin it includes PC-3, OVCAR-3, hep-G2, h-1299, HeLa, and MCF-7. Apoptotic potential is studied using the OVCAR-3 cell line. In-vitro cytotoxicity assay was conducted with the non-cancer cell lines HEK-293, L-929, hMSCs, and MCF-10A. Using mouse model, in-vivo animal toxicity was also carried out. The lichen extracts showed a good amount of phenolic and flavonoid content and high antioxidant potential. Based on the findings of the experiment, methanolic extracts of *A. ornatooides* showed higher immunomodulatory, anti-inflammatory and anticancer capabilities. In an in-vitro cytotoxicity test against the cancer cell line IC₅₀ value ranged from 38 to 78 µg/ml. Based on in-vivo toxicological evaluation and histopathological analysis, no significant toxicity was detected in-vitro cultured non-cancerous cells or in the liver or kidney tissue of mice.

© 2023 SAAB. Published by Elsevier B.V. All rights reserved.

Abbreviations: AO, Acridine Orange; ABTS, 2,2-Azino-Bis-(3-Ethylbenzothiazoline-6-Sulfonic Acid); BUBH, Bodoland University Botanical Herbarium; Bw, Bodyweight; CSIR-NBRI, National Botanical Research Institute; DPPH, 1,1-diphenyl-2,2-picrylhydrazil; DW, Dry weight; EC₅₀, Half-maximal effective concentration; Etr, ethidium bromide; FACS, Fluorescence-activated cell sorting; FRAP, Ferric reducing antioxidant power; GC–MS, Gas chromatography mass spectroscopy; h1299, Lungs cancer; HeLa, Cervical cancer; Hep-G2, Hepatic cancer; IC₅₀, Half-maximal inhibitory concentration; Kg, Kilogram; MCF-7, Breast cancer; mg, Milligram; ml, Milliliter; nm, Nanometre; OVCAR-3, Ovarian cancer; PC-3, Prostate cancer; TFC, Total flavonoid contents; TPC, Total phenolic contents; µg, Microgram

* Corresponding author.

E-mail address: rebeccadm@gmail.com (R. Daimari).

<https://doi.org/10.1016/j.sajb.2023.11.037>

0254-6299/© 2023 SAAB. Published by Elsevier B.V. All rights reserved.

1. Introduction

Oxidative stress, a phenomenon introduced by reactive oxygen species (ROS) or free radicals, is important for living organisms and cellular activities (Forcados et al., 2016). At normal physiological concentrations, they play a positive role in the signalling pathways (Alpay et al., 2015). The largest powerhouse of cells, mitochondria, can create ROS when generating adenosine triphosphate (ATP), where electrons react with the oxygen to form superoxide anions (Pisoschi and Pop, 2015). Numerous literatures confirmed that free radicals have a deep relationship with the human pathophysiological diseases. Moreover, oxidative stress is specifically well acknowledged to impair DNA molecules and regulate the progression of various cancers of the breast, lung, liver, colon, prostate, ovary, and brain,

including disorders and ageing (Saed et al., 2017; Hajam et al., 2022). Antioxidants, a possible self-protective agent, can be considered to neutralise oxidative damage caused by free radicals in human body, which discourages many chronic diseases (Kim et al., 2015). The natural product antioxidant can modify the behaviour of cancer cells by shifting their redox environment, which reduces their genetic unpredictability and therefore may be considered for use in cancer treatment (Nguyen-Trinh et al., 2022). Inflammation is also strongly associated with the onset and spread of cancer. Targeting inflammation is an appealing technique for both the prevention and treatment of cancer. Numerous conditions, such as bacterial and viral infections and autoimmune disorders, contribute to tumor-extrinsic inflammation, which in turn promotes the growth of cancer cells. On the other hand, cancer-elicited inflammation may be brought on by cancer-starting mutations and may result in malignant growths (Zhao et al., 2021a). Several strategies were elaborated in fighting cancer; the importance of chemotherapy is specified most of the time, and it is showing effectiveness against many cancer types. But the resistance to synthetic drugs limits successful results in most cases. The increased and uninhibited use of synthetic drugs has led to the discovery of new sources of natural products for the control and prevention of various diseases related to humans, animals and plants. It was well recognised that long-term use of a synthetic drug often causes resistance and overflowing side effects. As opposed to synthetic drugs, naturally formed bioactive compounds have more beneficial effects on the whole organism without causing unwanted effects. Moreover, the synthetic drug's incapability make deters their unanimous choice to distinguish between normal and cancerous cells. Hence, major focus is being given to explore for better and safer antioxidants of natural origin that may raise the efficacy of cancer treatment. In the examination of new bioactive preparations of natural products, lichens have been the focus of many research teams. Lichens are slow-growing, self-supporting, stable, symbiotic associations composed of a mycobiont (fungus) and a photobiont (algae) (Calcott et al., 2018). It has the ability to grow as scattered patches on rocks, outcrops, soils and tree trunks or shrubs and able to tolerate extreme environmental conditions hostile to the survival of the individual partners. Lichens have been found to produce a wide variety of secondary substances that are unique to higher groups of plants. More than 1050 secondary metabolites are well known for their remarkable range of biological activities, including antifungal, antineoplastic, analgesic, anti-inflammatory, antimicrobial, anti-viral, antioxidant, antipyretic, antitumor, enzyme inhibitor, and herbicidal (Stocker-Wörgötter, 2008; Pham et al., 2021; Gandhi et al., 2022). These lichen substances are usually deposited on the surface of mycelium cells and are mostly water-insoluble (Zhao et al., 2021b). There are inadequate number of literatures where the mechanisms of action against cancer cell lines have been studied (Pradhan et al., 2022). The molecular mechanism of cell death by lichen compounds includes cell cycle arrest, apoptosis, and inhibition of angiogenesis (El-Garawani et al., 2019; Yurdacan et al., 2019). Therefore, much consideration has been given to detecting the natural antioxidant products for their capacity to protect organisms from being damaged by oxidative stress. Hence, the present study was undertaken to explore the antioxidant, immunomodulatory, anti-inflammatory, and anticancer activities of *Anzia ornatoides* extract. It belongs to family *Parmeliaceae* and is characterized by thallus foliose, corticolous, smooth, dorsiventral, lobulate, heteromerous, lower side spongy, with reticulate anastomosing thick, corticated on upper side, isidia simple, concolorous, spreading on the thallus.

The lichen *A. ornatoides* was collected during the month of January 2022 from Ultapani Forest Range, Kokrajhar district, Assam, in the Eastern Himalayan region, situated in the foothills of Bhutan. Determination of the investigated lichen was accomplished in CSIR-NBRI, Lucknow with the standard key (Awasthi, 2007) and deposited in the herbarium of CSIR-NBRI, Lucknow, 63364 (LWG), and Department of

Botany, Bodoland University, Kokrajhar, Assam, 2022–0101 (BUBH). *A. ornatoides* contains the secondary substances lobaric, sublobaric, stictic acids, atranorin, proprotocetraric, and fumaprotocetraric acid (Awasthi, 2007; Singh and Sinha, 2010).

2. Materials and methods

2.1. Preparation of lichen extract

The lichen specimen, *A. ornatoides*, was air dried at room temperature and stored in paper bags. Then the material was grinded in a mixture grinder. Finely, 50 g of dried ground thalli were extracted with 1000 ml of hexane, diethyl ether, ethyl acetate, methanol, and water in increasing polarity using Soxhlet apparatus for 8–16 h. Thereafter, the crude extracts were concentrated in a reduced-pressure rotary evaporator (IKON, IK-154) and preserved at 4 °C for further experiments.

The dry extracts of *A. ornatoides* prepared in different five solvents had various colors, depending on the other organic compounds extracted in each solvent. The obtained yields are reported in Table 1

2.2. Antioxidant activity of *A. ornatoides*

2.2.1. Total phenolic contents

The total soluble phenolic compounds in extracts were determined by the Folin-Ciocalteu reagent (Slinkard and Singleton, 1997), using gallic acid as a standard phenolic compound. Briefly, 50 μ l of the extracts (5 mg/ml in 5 % DMSO) in a test tube were diluted with water (1.8 ml) and 1 ml of Na_2CO_3 (10 %) was mixed to the extract thoroughly. After 2–3 min, 150 μ l of Folin-Ciocalteu reagent was added, and the mixtures were kept for 10–20 min at room temperature. The absorbance was taken at 765 nm in a UV–VIS spectrophotometer (UV-1900i, Shimadzu) against a blank (all the reactions except the extract). The concentration of phenolic content in the extracts was estimated as milligrams of gallic acid equivalent (GAE) per gram of dry weight (mg GAE g^{-1}) by using an equation obtained from gallic acid standard graph.

2.2.2. Total flavonoid contents

The total flavonoid content was determined according to the method of Dowd (Meda et al., 2005). Briefly, 50 μ l of the extract solution (5 mg/ml in 5 % DMSO) was diluted in distilled water (1.95 ml) and 1 ml of aluminium trichloride (2 % AlCl_3 in methanol) was added to it. The mixtures were placed at room temperature for about 10–12 min. Thereafter, absorbance was measured at 415 nm in a UV–VIS spectrophotometer (UV-1900i, Shimadzu). The negative control (all the reactions without extract) was used as a blank. The concentration of flavonoid content was estimated as milligrams of quercetin equivalent (QE) per gram of dry weight (mg QE g^{-1} DW) using an equation obtained from the quercetin graph.

2.2.3. Phosphomolybdenum assay

The phosphomolybdenum method was used to evaluate total antioxidant compounds (Prieto et al., 1999). The assay is used for the

Table 1

The temperature values for refluxing at Soxhlet, extraction yield and colors of *A. ornatoides* dry extracts using different solvents.

Extracts	Temperature (°C)	Yield (%)	Color after extraction
Hexane	68	0.6	Olive yellow
Diethyl ether	34.6	4.56	Yellowish green
Ethyl acetate	77.1	7.33	Greenish yellow
Methanol	64.7	13.83	Brownish yellow
Water	100	18.26	Reddish brown

reduction of Mo(VI)-Mo(V) by antioxidant compound and subsequent formation of a green phosphate Mo(V) complex at low pH. Briefly, in a 3 ml vial, 0.1 ml of aliquot solution (5 mg/ml in 5 % DMSO) with 1 ml of reagent solution (0.6 M sulphuric acid, 28 mM sodium phosphate and 4 mM ammonium molybdate) and diluted upto 3 ml with distilled water. The mixture solution was incubated for 90 min in water bath at 95 °C. After cooling to room temperature, the absorbance was measured at 765 nm in a UV–VIS spectrophotometer (UV-1900i, Shimadzu) against a blank (0.1 ml of methanol in place of extract). The results were estimated from the standard ascorbic acid graph as milligrams of ascorbic acid equivalent (AAE) per gram of dry weight (mg AAEg⁻¹DW).

2.2.4. Ferric-reducing antioxidant power assay

The reducing power of the extracts was determined by the method of Oyaizu (Oyaizu, 1986), using ascorbic acid as a standard compound. Various concentrations of the extracts (5 mg/ml in 5 % DMSO), 10–50 μ l were mixed with 1 ml of phosphate buffer (0.2 M, pH 6.6) and 1 ml of 1 % potassium ferricyanide [K₃Fe(CN)₆]. After 30 min of incubation at 50 °C in a water bath, 1 ml of 10 % trichloroacetic acid was added to the mixture to rest the reaction, and it was centrifuged at 3000 g for 10 min. Then, 1 ml of supernatant was mixed with distilled water (1.5 ml) and FeCl₃ (0.5 ml, 0.1 %); and absorbance was measured at 700 nm in a UV–VIS spectrophotometer (UV-1900i, Shimadzu) against a blank (all the reaction agents without extract). The reducing power is increased when the reaction mixture shows higher absorbance.

2.2.5. Scavenging DPPH radicals

The free radical scavenging activity of the extracts was determined by 1,1-diphenyl-2,2-picrylhydrazil. The method was previously used by some authors (Gadow et al., 1997; Dorman et al., 2004). Different concentrations of extracts (5 mg/ml in 5 % DMSO) and standards, namely 10–50 μ l, were prepared in test tubes, and 2 ml of a methanolic solution of the DPPH radical (0.05 mg/ml) was added to it and diluted up to 3 ml with distilled water. Then the mixture was kept at room temperature for about 30 min, and absorbance was measured at 517 nm against a blank (methanol) in a UV–VIS spectrophotometer (UV-1900i, Shimadzu). It was calculated with the following equation:

$$\text{DPPHscavengingeffect(\%)} = (A_0 - A_1/A_0) \times 100$$

where A₀ is the absorbance of the control (2 ml of methanolic solution of DPPH radical and 1 ml of 5 % DMSO) and A₁ is the absorbance of the reaction mixture or standard (ascorbic acid). The results of inhibitory activity towards DPPH are presented as EC₅₀ values.

2.2.6. ABTS assay

The antioxidant activity of the extracts was measured by the 2,2'-Azino-bis-(3-ethylbenzothiazoline-6-sulfonic acid) ABTS⁺ radical cation decolorization assay (Re et al., 1999). The aqueous solution of 7 mM ABTS⁺ and 2.4 mM potassium persulfate was kept in the dark for 12–16 h at room temperature to produce ABTS. This radicle was constant when stored in the dark at room temperature for more than two days. The ABTS solution was diluted in ethanol (about 1:84 v/v) and balanced at 30 °C for the absorbance of 0.70000.02 at 734 nm. Then, 2 ml of diluted ABTS⁺ solution was added to the different sample concentrations (5 mg/ml in 5 % DMSO) or standard trolox (10–50 μ l) and diluted up to 3 ml with distilled water. After incubation for 30 min at room temperature, the absorbance was recorded at 734 nm using a UV–VIS spectrophotometer (UV-1900i, Shimadzu) against a blank (ethanol). The percentage of inhibition of ABTS was calculated with the following formula:

$$\text{ABTScavengingeffect(\%)} = (A_0 - A_1/A_0) \times 100$$

Where, A₀, an absorbance of control and A₁, an absorbance of standard or extracts. The results of the inhibitory activity of ABTS are presented as EC₅₀ values.

2.2.7. Determination of the inhibitory activity toward lipid peroxidation

The antioxidant activity of the extracts was determined by the thiocyanate method (Hsu et al., 2008). The 0.5 ml of stock solution (5 mg/ml of extracts in 5 % DMSO) was added to the linoleic acid emulsion (2.5 ml, 40 mM, pH 7.0). The mixture of 0.2804 g Tween 20 as an emulsifier in 50 ml of 40 mM phosphate buffer, pH 7.0, was prepared for a linoleic acid emulsion and placed at 37 °C in the dark for about 72 h. Then, a serially 10–50 μ l aliquot of the reaction solution was mixed with 2.3 ml of ethanol, 50 μ l of FeCl₂ (20 mM), and 50 μ l of ammonium thiocyanate (30 %), and stirred for 3 min before being measured at 500 nm using a UV–VIS spectrophotometer (UV-1900i, Shimadzu). Ascorbic acid was used as a reference compound. The inhibition percent of linoleic acid peroxidation was calculated with the given formula:

$$\% \text{inhibition} = (A_0 - A_1/A_0) \times 100$$

Where, A₀, an absorbance of control and A₁, an absorbance of standard or extracts. The results of inhibitory activity toward lipid peroxidation are presented as EC₅₀ values.

2.3. Anticancer activity of *A. ornatoides*

2.3.1. Cell culture and reagents

The cancer cell lines prostate cancer (PC-3), ovarian cancer (OVCAR-3), hepatic cancer (hep-G2), lungs cancer (h-1299), cervical (HeLa) and breast cancer (MCF-7) were obtained from the National Cell Repository, NCCS, Pune, India. The cell lines were preserved in 5 % CO₂ culture conditions at 37 °C, supplemented with RPMI-1640, 10 % foetal bovine serum, and antibiotics (penicillin and streptomycin). The cells were grown in T75 culture flask with complete RPMI-1640 medium.

2.3.2. Determination of cytotoxicity by MTT assay

The cancer cell lines PC-3, OVCAR-3, MCF-7, HeLa, Hep-G2, and h1299 were seeded in 96-well plates (3 × 10⁴ cells/well) and incubated for 24 h. Then, the cells were treated with a 5 μ g/ml to 160 μ g/ml (dissolved in 1 % DMSO) concentration of the extracts and again incubated for 72 h. At the end of experiment MTT (3-[4,5-dimethylthiazol-2-yl]-2,5 diphenyl tetrazolium bromide), 0.5 mg/ml (dissolved in 1 % DMSO) was added to each well and incubated for 3 h followed by discard of content and addition of 100 μ l DMSO and absorbance was measured at 570 nm using ELISA plate reader (Saluja et al., 2020; Meher et al., 2021a; Meher et al., 2023). The IC₅₀ value of the extract against the cell was measured by the AAT bio quest calculator.

2.3.3. Fluorescence imaging for the detection of apoptosis

Acridine Orange and ethidium bromide stains were used to study cells with fluorescence microscopy. OVCAR-3 were grown on 6-well plates containing coverslips and treated with methanolic extract at IC₅₀ concentration for 72 h. After incubation, the plates were fixed in 3 % formaldehyde and washed with phosphate buffered saline (PBS), stained with AO and Etbr at a concentration of 10 μ g/ml, and washed after 10 min using PBS to remove unbound stain. Coverslip was mounted on a slide, and images were captured using a confocal microscope (Carl Zeiss). Apoptotic cells were identified based on their shape in comparison to untreated cells (Meher et al., 2021b; Mir et al., 2023).

2.3.4. Flow cytometry for the detection of apoptosis

For induction of apoptosis, OVCAR-3 were treated with the IC₅₀ concentration of methanolic extract and Berberine separately and incubated for 48 h. After inducing apoptosis, cells were labelled with Hoechst 33342 (15 μ g/ml) for 45 min. With 30,000 events recorded, Ho33342 was stimulated by UV or 405 nm lasers, and emission was captured at 440/40 nm.

2.4. Cell viability assay of macrophages to detect immunomodulatory effects

The macrophage cell (RAW 264.7) was treated with different concentrations of the extracts (5 $\mu\text{g/ml}$ –160 $\mu\text{g/ml}$) and incubated for 72 h before being subjected to the SRB (Sulforodamine B assay), as previously reported. Briefly, 3×10^3 cells/well were seeded on a 96-well culture plate and incubated for 24 h, followed by treatment of the extract and further incubation for 72 h. At the end of the experiment, SRB (0.5 %) was added to each well and incubated for 30 min, followed by washing and the addition of 1 % acetic acid, and absorbance was measured at 510 nm using an ELISA plate reader (Meher et al., 2018; Behera et al., 2023). The IC_{50} value of the extracts against the cell was measured by the AAT Bioquest software method.

2.5. Detection of anti-inflammatory effect

2.5.1. Assessment of cellular ROS

Invitrogen CellROX[®] Green Reagent (Invitrogen, Carlsbad, CA, USA) was used to measure the cellular ROS concentration in accordance with the manufacturer's recommendations. In a 24-well plate, RAW 264.7 macrophage cells were planted for 24 h. LPS (0.5 $\mu\text{g/ml}$) was added to the cells for 6 h with or without a methanolic extract of hydrilla. CellROX green dye was then used to stain the cells for 15 min at 37 °C. Using an automated microscope, the stained ROS were photographed after being cleaned with 1X PBS.

2.5.2. Assessment of NO_2 in macrophages

Meter[™] Fluorimetric Intracellular Nitric Oxide Assay Kit was used to determine intracellular nitric oxide according to the manufacturer's suggestion. The macrophage cell line (Raw 264.7) was seeded in a 24-well black-walled culture plate with a clear bottom. The cells were incubated with Nitrixyte[™] Orange and treated with LPS (1 $\mu\text{g/ml}$) alone or LPS with a methanolic extract of hydrilla for 24 h. The fluorescence signal was measured with a fluorescence microscope.

2.6. Toxicity analysis

2.6.1. In-vitro toxicity analysis

The cytotoxicity evaluation was performed using the normal cell lines human embryonic kidney cell line (HEK-293), murine fibroblast (L-929), human mesenchymal cells (hMSCs), and human breast epithelial cell line (MCF-10A). In brief, cells were allowed to grow in culture medium (MEM, DMEM) supplemented with 10 % FBS, 1 % penicillin/streptomycin, with maintenance of temperature at 37 °C and 5 % CO_2 . In a 96-well plate, the cells were seeded at a density of 5×10^3 cells/well and treated with increasing concentrations (10 $\mu\text{g/ml}$ to 400 $\mu\text{g/ml}$) of methanolic extract for 72 h. The cells were then stained with 0.56 % sulphorodamine B in 1 % acetic acid. To remove unbound stains by washing, 1 % acetic acid was used. 10 mM Tris base with a pH of 10.5 was added to the 96-well plate containing fixed cells with protein-bound stain, and the absorbance was measured at a 495 nm wavelength using a Bio Red 96-well plate reader. The IC_{50} values for the extract were calculated from the plate reader data by using an online IC_{50} value calculator (AAT Bioquest, Inc., Sunnyvale, CA, USA).

2.6.2. In-vivo toxicity analysis

The Institutional Animal Ethics Committee of Siksha O' Anusandhan Deemed to be University accepted all of the study's experimental protocols (Protocol IAEC/SPS/SOA/18/2019), which were carried out in accordance with the requirements of the Government of India's "Committee for Control and Supervision of Experiments on Animals." Nude mice ages 8 to 10 weeks were kept in the animal care facility. The experimental animals were randomly divided into 5 groups; each group consists of 5 animals. Group I (the control) was given a daily gavage of vehicle solution (acidified water, pH 4.0) only,

whereas groups 2–5 were treated with 500–2000 mg/KgBw. On day 30, animals were anaesthetized with ketamine (20 mg/kg i.p.) at the end of the study. The animals were sacrificed after being anaesthetized, and the essential organs, such as the liver and kidney, were excised and histologically examined. Tissues were paraffin-embedded, sectioned and haematoxylin and eosin stained. To assess toxicity, the tissues were examined under a microscope.

2.7. GC–MS analysis

For the GC–MS analysis, the methanolic extract of the sample was carried out with a Perkin Elmer (USA) GCMS instrument, Model Clarus 680 d amp, CaluMS,600C MS comprising a liquid auto-sampler. Turbo-Mass Ver 6.1.2. software has been used and the peaks were analysed by data analysis software NIST-2014. The capillary column used was "Elite-5MS" having dimensions-length-60 m, ID-0.25 mm and film thickness-0.25 μm . The 5 % diphenyl 95 % dimethyl polysiloxane is used for the stationary phase. In the GC-Protocol, helium gas (99.99 %) was used as a carrier gas (i.e., mobile phase) at a flow rate of 1 ml/min. An injection volume of 2 μl was employed in splitless mode. Injector temperature is 280 °C, and ion-source temperature is 180 °C. The oven temperature was programmed at 60 °C (for 1 min), with an increase at the rate of 7 °C/min to 200 °C (hold for 3 min), then again increased at a rate of 10 °C/min to 300 °C (hold for 5 min). The total run time is ~39 min. Solvent delay was kept for 8 min. A MS protocol mass spectral measurement was taken in electron impact positive (EI+) mode at 70 eV. A solvent delay of 8 min was there for MS scan. Mass range i.e., m/z range is 50–600 amu. Interpretation of the peaks appeared in the GC chromatogram were done by library search of the mass spectrum of corresponding peaks using the database software of National Institute Standard and Technology-2014 (NIST-2014). The mass spectra of unknown components was compared with the known components of the NIST library, and compounds were identified by name, molecular weight, and empirical formula.

2.8. Statistical analysis

Statistical analysis was performed with Excel and Kruskal-Wallis Anova analysis in Origin 2020b. All values are represented as the mean \pm SE of three parallel measurements. Differences were considered significant when $p < 0.05$ and $p < 0.01$. The IC_{50} value ($\mu\text{g/ml}$) was calculated using the AAT Bioquest IC_{50} value calculator.

3. Results and discussion

3.1. Total phenolic contents

The total phenolic compounds of the extracts were calculated (Fig. 1) as the gallic acid equivalent (GAE) using an equation obtained from a standard gallic acid graph ($y = 0.0064x + 0.024$, $R^2 = 0.9961$). The results of the study showed the phenolic compounds of the tested extracts varied from 2.93 ± 0.13 mg GAE g^{-1}DW to 8.27 ± 0.13 mg GAE g^{-1}DW . *A. ornatooides* showed the highest phenolic

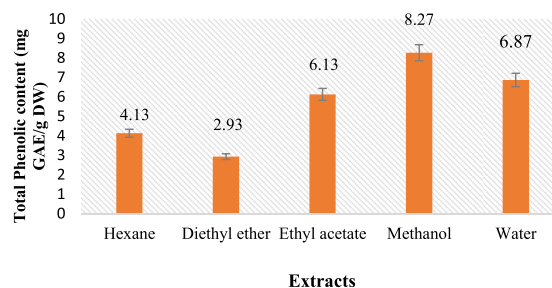


Fig. 1. Total phenolic content (mg GAE/g DW) of different extracts.

content with methanol extract, and the lowest phenolic content was shown in diethyl ether extract. The variation increased in the order of methanol>water>ethyl acetate>hexane>diethyl ether. There was a statistically significant different at $P < 0.01$ (Table 6).

The result indicated phenolic compounds were accumulated more in polar solvents than in non-polar solvents. The variation could have been attributed to different solvent polarities (Vyas et al., 2015). Phenolic compounds contain hydroxyl groups, which are significant constituents responsible for antioxidant activity and free radical terminators. These compounds are the chief agents that can donate hydrogen to free radicals and break the chain reaction of lipid oxidation at the initial step. Phenolic contents can scavenge the development of free radicals in the human body due to the presence of their hydroxyl groups (Nur et al., 2019).

3.2. Total flavonoid contents

The flavonoid compounds were determined as the quercetin equivalent using an equation obtained from a standard graph ($y = 0.009x - 0.046$, $R^2 = 0.9992$). The results of the study showed the flavonoid compounds of the tested extracts varied from 1.53 ± 0.07 mg QE g^{-1} DW to 2.00 ± 0.00 mg QE g^{-1} DW. As shown in Fig. 2, the maximum flavonoid contents were identified with the methanol extract, while diethyl ether showed the lowest flavonoid content. The variation increased in the order of methanol>hexane>water>ethyl acetate>diethyl ether. There was a statistically significant different at $P < 0.01$ (Table 6).

Flavonoid compounds were also accumulated in polar rather than non-polar solvents. Flavonoids, a most important natural phenol, possess a broad spectrum of chemical and biological activity, including radical-scavenging properties. It is known to be polyphenolic compounds comprising two phenyl rings linked by a propane bridge, resulting in a characteristic 15-carbon (C6-C3-C6) flavan skeleton (Neilson et al., 2017). It can be regarded as a class of phenolic compounds with low molecular weight that can neutralise the free radicals in the human body; the activity depends on the number and location of the OH group, which are related to the ability of these compounds to donate electrons (Vyas et al., 2015; Zawawi et al., 2021).

3.3. Phosphomolybdenum assay

The total antioxidant compounds were estimated as the ascorbic acid equivalent using an equation obtained from a standard ascorbic acid graph ($y = 0.0031x - 0.011$, $R^2 = 0.9981$). The results of the study showed antioxidant compounds of the tested varied from 2.73 ± 0.67 mg AAE g^{-1} DW to 13.13 ± 0.67 mg AAE g^{-1} DW.

As shown in Fig. 3, the most abundant antioxidant compounds were identified in the water extract, while ethyl acetate showed the lowest antioxidant content. The variation increased in the order of water>methanol>hexane>diethyl ether>ethyl acetate. There was a statistically significant different at $P < 0.01$ (Table 6). The antioxidant compounds can counteract the free radicals that do not have a partner and become unstable with high reactivity (Saroyo and Nur, 2020).

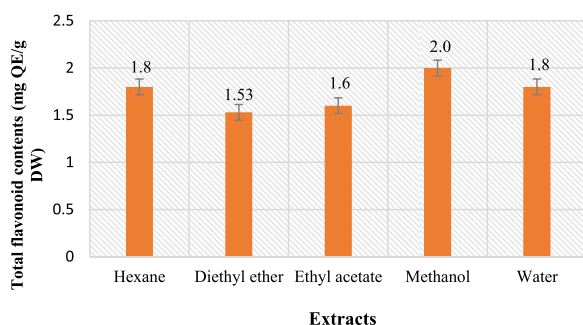


Fig. 2. Total flavonoid content (mg QE/g DW) of different extracts.

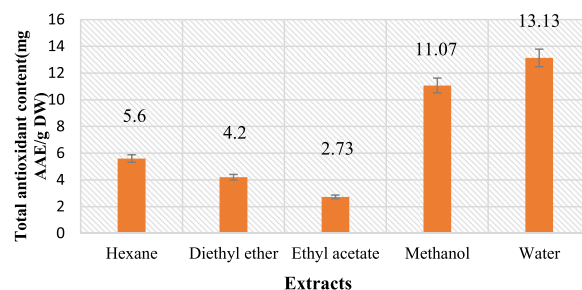


Fig. 3. Total antioxidant compounds by phosphomolybdenum method (mg AAE/g DW) of the different extracts.

3.4. Ferric-reducing antioxidant power (FRAP) assay

The FRAP activity were measured as the ascorbic acid equivalent using an equation obtained from a standard ascorbic acid graph ($y = 0.0119x - 0.053$, $R^2 = 0.9978$). The results of the reducing power assay of the extracts are presented in Fig. 4. Higher absorbance of the reaction mixtures indicates greater reducing power. Measured values of the absorbance varied from 1.4 to 3.0. Among the tested extracts, methanol showed the highest reducing power, while hexane showed the lowest reducing power. The reducing power of the extracts decreased in the following order: methanol>ethyl acetate>diethyl ether>water> hexane. There was a statistically significant different at $P < 0.01$ (Table 6).

The reducing power of the compound may serve as a significant indicator of its potential antioxidant activity. The reducing potential is generally connected with the presence of its reductons, is made on breaking of free radical chain by donating a hydrogen atom. The reduction of ferrous ions (Fe^{3+}) to ferric ions (Fe^{2+}) is observed by the intensity of the blue-green resultant solution, which absorbs at 700 nm. The presented result shows the ferric reducing power activity of extracts is owing to the presence of their polyphenol compounds, which may act in a similar way to reductons by donating electrons and reacting with free radicals to convert them into more stable products and terminate chain reactions of free radicals. In this assay, there is an electron transfer mechanism present that could affect the activity of phenolic compounds present in the extracts (Dobros et al., 2022).

3.5. Scavenging DPPH radicals

The percentage of scavenging DPPH radicals of the different extracts is shown in Table 2. Fig. 5A represents the EC_{50} data of the DPPH scavenging activities of the extracts. There was a statistically significant difference between extracts and concentration at $p < 0.05$, $P < 0.01$ (Table 7a & 7b). The method has been employed for the evaluation of free radical scavenging activity of several natural product extracts (Mbaoji and Nweze, 2020).

This DPPH assay is being used for the preliminary test which provides an information on the reactivity of test extract compounds with a stable free radical gives purple colour strong absorption

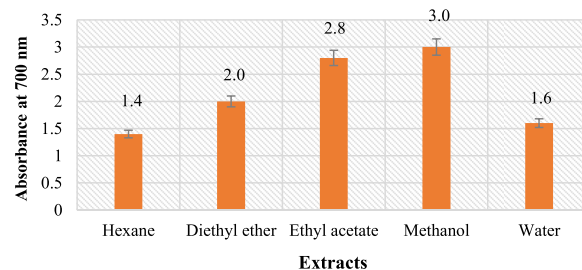
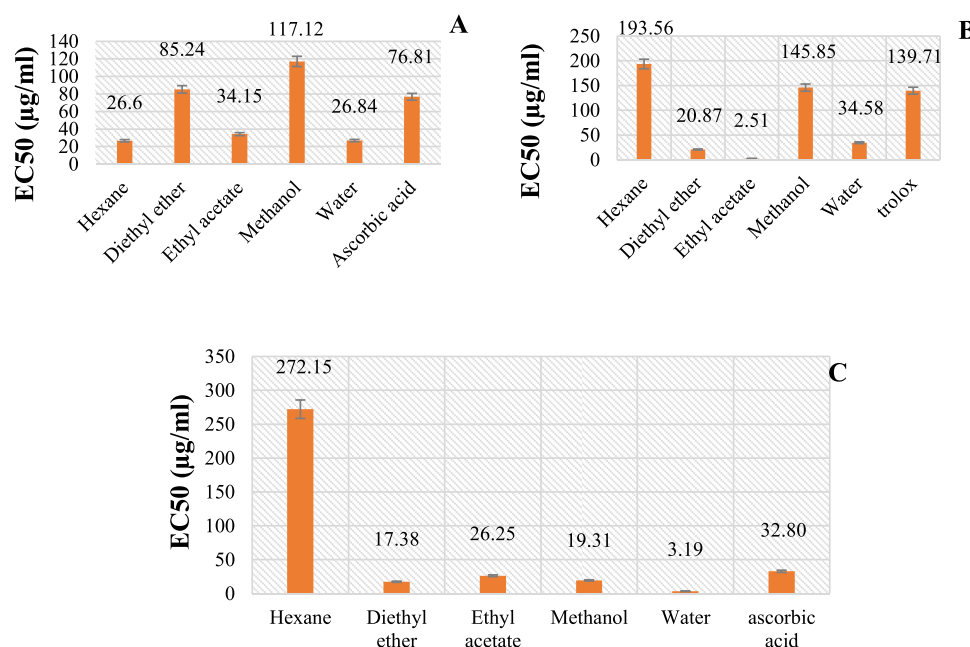


Fig. 4. Ferric-reducing antioxidant power (FRAP) (mg AAE/g DW) of different extracts.

Table 2
Percentage scavenging rate of DPPH free radicals by extracts.

Concentration ($\mu\text{g/ml}$)	Extracts				
	Hexane	Diethyl ether	Ethyl acetate	Methanol	Water
10	10.30 \pm 1.00	11.80 \pm 0.85	15.44 \pm 0.16	11.65 \pm 0.73	5.60 \pm 0.27
20	10.92 \pm 0.74	14.86 \pm 1.18	21.81 \pm 0.84	18.04 \pm 0.54	10.77 \pm 0.31
30	12.17 \pm 0.16	18.80 \pm 0.32	27.19 \pm 0.11	22.17 \pm 0.40	14.01 \pm 0.26
40	12.51 \pm 0.12	24.13 \pm 0.57	30.71 \pm 0.91	28.02 \pm 0.15	17.16 \pm 0.05
50	13.06 \pm 0.21	29.42 \pm 0.03	33.85 \pm 0.38	33.27 \pm 1.65	18.47 \pm 0.11

**Fig. 5.** A: 2,2-diphenyl-1-picrylhydrazyl radical; B: 2,2'-azino-bis-(3-ethylbenzothiazoline-6-sulfonic acid) assay; C: Inhibitory activity towards lipid peroxidation; EC₅₀: Concentration of the sample providing 50 % effectiveness.

maximum band at 517 nm when it is reduced by the extract compound there will be a decrease in absorbance and discolouration from purple to yellow. It has been reported that the antioxidant activity of this lichen might be attributed to the presence of the hydroxyl functional group of phenolic compounds having redox properties (Borkatky et al., 2013).

3.6. ABTS scavenging capacity

The results of the percentage ABTS scavenging activities of the extracts are presented in Table 3. There was a statistically significant difference between extracts and concentration at $P < 0.01$ (Table 8a & 8b). Fig. 5B represents the EC₅₀ data of the ABTS scavenging activities of the extracts. Highest EC₅₀ value was observed in hexane extract while lowest in ethyl acetate.

ABTS have been also operated for the evaluation of free radical scavenging activity of extracts using trolox as a standard, which

stabilizes the free radicals through proton donors and provides lipophilic and hydrophilic compounds through proton donors and provides lipophilic and hydrophilic compounds (Chohra et al., 2020).

3.7. Inhibitory activity towards lipid peroxidation

The results of inhibition activity of lipid peroxidation by the extracts are summarized in (Table 4). There was a statistically significant difference between extracts and concentration at $P < 0.05$, $P < 0.01$ (Table 9a & 9b). Fig. 5C represents EC₅₀ data for the lipid peroxidation inhibition activities of the extracts. Highest EC₅₀ value was observed in hexane extract while lowest in water extract. The antioxidant activity has a synergetic action of various compounds that can work in free radical scavenging and directs inhibition of lipid peroxidation (Lompo et al., 2016).

The effects of different concentrations of the extracts on lipid peroxidation, as shown in Table 4, exhibited concentration-dependent

Table 3
Percentage scavenging rate of ABTS radicals by extracts.

Concentration ($\mu\text{g/ml}$)	Extracts				
	Hexane	Diethyl ether	Ethyl acetate	Methanol	Water
10	9.85 \pm 1.32	15.00 \pm 1.32	42.98 \pm 0.46	6.33 \pm 1.40	6.85 \pm 0.13
20	21.98 \pm 1.74	32.48 \pm 3.09	58.25 \pm 0.65	15.78 \pm 0.43	9.72 \pm 0.06
30	33.33 \pm 0.57	43.77 \pm 1.14	59.30 \pm 0.11	24.33 \pm 0.34	12.65 \pm 0.07
40	42.99 \pm 0.46	51.73 \pm 0.75	60.73 \pm 0.17	32.36 \pm 0.28	26.74 \pm 0.46
50	57.66 \pm 0.52	53.69 \pm 1.13	65.56 \pm 0.69	41.62 \pm 0.13	30.46 \pm 1.94

Table 4
Percentage scavenging rate of lipid peroxidation radicals by extracts.

Concentration ($\mu\text{g/ml}$)	Extracts				
	Hexane	Diethyl ether	Ethyl acetate	Methanol	Water
10	5.38 \pm 0.53	24.73 \pm 0.54	11.83 \pm 0.53	25.27 \pm 0.54	31.19 \pm 0.53
20	39.25 \pm 1.07	45.16 \pm 2.46	23.12 \pm 1.94	49.46 \pm 1.42	60.21 \pm 1.08
30	47.85 \pm 1.08	56.45 \pm 0.93	48.93 \pm 0.54	62.37 \pm 2.99	63.44 \pm 0.54
40	57.52 \pm 0.54	60.22 \pm 0.54	57.52 \pm 0.54	73.65 \pm 0.54	66.13 \pm 0.00
50	80.65 \pm 0.93	62.90 \pm 0.93	66.13 \pm 1.61	77.42 \pm 5.30	72.58 \pm 0.00

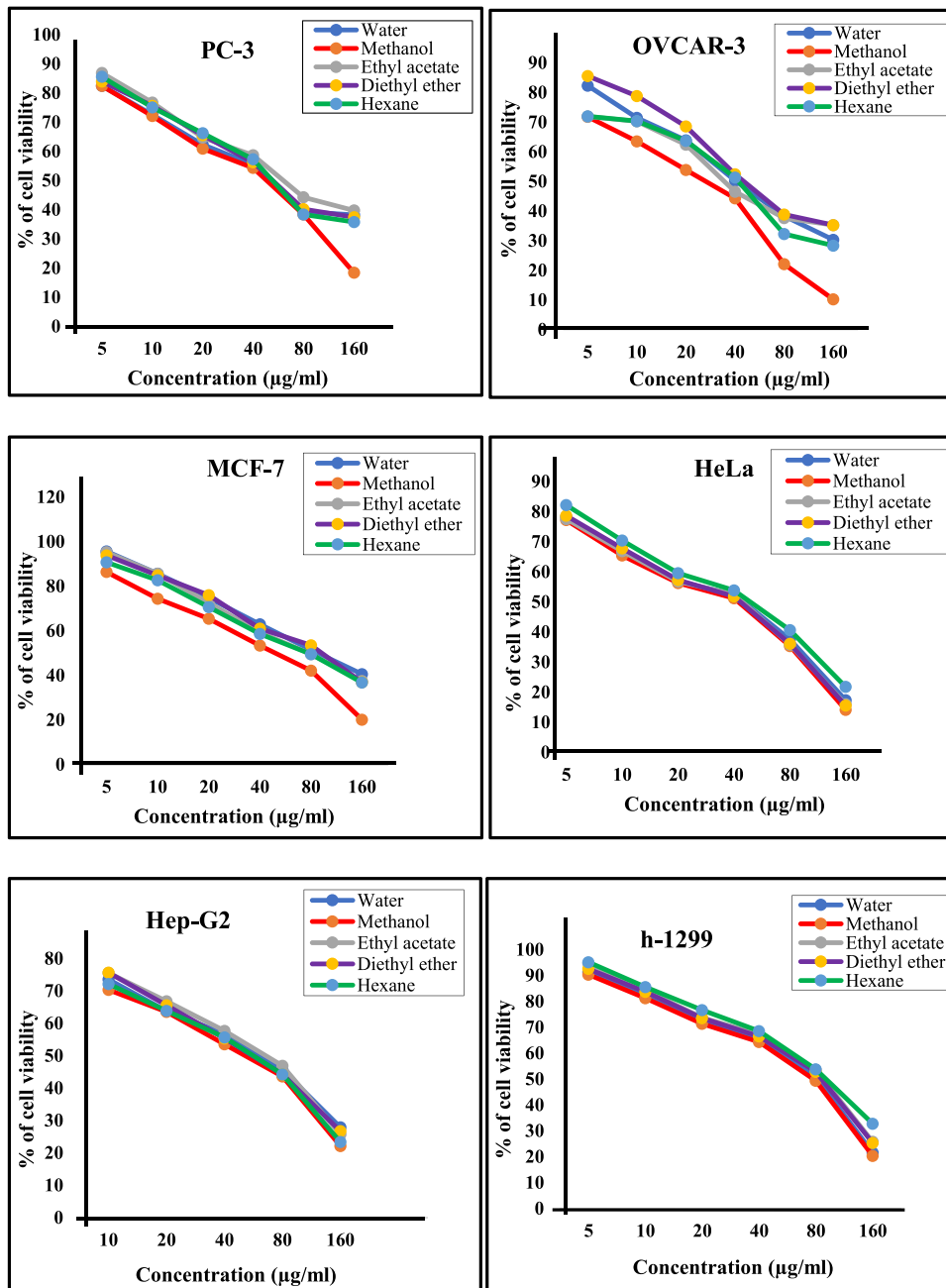


Fig. 6. Inhibition of proliferation of cancer cells against all the extracts. Different solvent extracts hexane, diethyl ether, ethyl acetate, methanol, and water used to compare among the cell lines. The figure contains multiple cancer cell types: PC-3, OVCAR-3, MCF-7, HeLa, Hep-G2, and h-1299. Each of these abbreviations represents a specific type of cancer cell line used in the experiment. The Y-axis of the figure represents the measure of inhibition of proliferation, which has been presented as a percentage of growth rate, and showed the effectiveness of methanolic extract at inhibiting cancer cell growth. The X-axis represents the increasing concentration of extract in specific solvent, data points or curves, each representing a different cancer cell line. These curves or data points show the inhibition of cancer cell proliferation varies with increasing concentration of extract for each cell line.

lipid peroxidation inhibition and were significant at higher concentrations. Lipid peroxidation method is a toxicological process, which is responsible for the excessive production of reactive oxygen species causes modification of lipoprotein, DNA sequences and protein (Ananthi et al., 2015).

3.8. Evaluation of cytotoxicity potential

The effectiveness of lichen extracts against the cancer cell lines PC-3, OVCAR-3, MCF-7, HeLa, Hep-G2, and h1299 was investigated (Fig. 6). The extract's cytotoxicity potential was tested at doses ranging from 5 $\mu\text{g/ml}$ to 160 $\mu\text{g/ml}$. In studies, the methanol extract suppressed maximum cancer cell growth compared to other extracts (Fig. 6), finally leading to apoptosis; and cell death effectiveness was directly proportional to the concentration of the extract. The cell line OVCAR-3 exhibits a high induction of cancer cell death (Fig. 6), therefore more investigation was performed with it. The cytotoxicity of the cell line was concentration and time-dependent, as shown by the IC_{50} value (Fig. 7). The IC_{50} value for PC-3, OVCAR-3, MCF-7, HeLa, HepG2, and h1299 was 52, 38, 48, 47, 52, and 78 $\mu\text{g/ml}$.

It is important to note that preliminary screening was carried out with multiple cancer cell lines with different solvent extract to evaluate its potential. From the screening results, the methanol extract showed promising effects on OVCAR-3, a well-established ovarian cancer cell line. As ovarian cancer is a significant health concern, research on potential treatments can have a substantial impact in this type of cancer. Subsequently, further studies were conducted using specific OVCAR-3 cell line with methanol extract. This approach allowed for more in-depth and targeted research on the selected cell line while also conserving resources and time.

3.9. Immunofluorescence imaging to detect apoptosis

Ao and EtBr staining were used to test the efficacy of the methanol extract to induce apoptosis. As the confocal image distinguishes, control cells exhibited a uniform nucleus, whereas apoptotic cells were

disintegrated (Fig. 7). After 48 h of treatment with extract, all of the treated cells displayed nuclear condensation.

3.10. Flow cytometry and confocal analysis for apoptosis

Apoptosis was generated to learn more about how cells die in response to the methanol extract. Only after apoptosis, when membrane permeability is reduced, a cell-impermeant DNA-binding fluorescent dye (Hoechst) can easily penetrate the cells. Confocal imaging and FACS analysis were used to quantify a significant number of apoptotic cells. After being treated with the IC_{50} dose of methanol extract, apoptotic cells against OVCAR-3 were analysed by the confocal microscopy and flow cytometry. A flow cytometry representative (Fig. 8) is included in the illustration. Only a few apoptotic (5 %) cells were found in the untreated cell, which was most likely background cell death due to normal cell culture damage. In contrast, when OVCAR-3 was treated with the extract, the fraction of apoptotic cells was 55 %, which was greater than untreated.

3.11. Evaluation of immunomodulatory activity

Methanol extract of *A. ornatooides* showed the highest immunomodulatory activity compared to the other extracts (Fig. 9). Consequently, the potency of methanolic extracts in favour of macrophage cell line (Raw 264.7) proliferation shows the effectiveness of the extract in a concentration-dependent manner.

Immunomodulators are substances that can enhance or regulate the immune system's response. Lichen-derived compounds may help modulate the immune system to better recognize and eliminate cancer cells. Some lichen extracts or compounds have shown potential as anticancer agents in laboratory studies. These effects are attributed to various mechanisms, including antioxidant properties, apoptotic inducer, anti angiogenic, anti-inflammatory properties (Dar et al., 2022; Adenubi et al., 2022).

3.12. Evaluation of anti-inflammatory activity

Further effectiveness of the methanolic extract on the (Raw-264.7) cell line towards ROS and NO_2 , was also investigated which

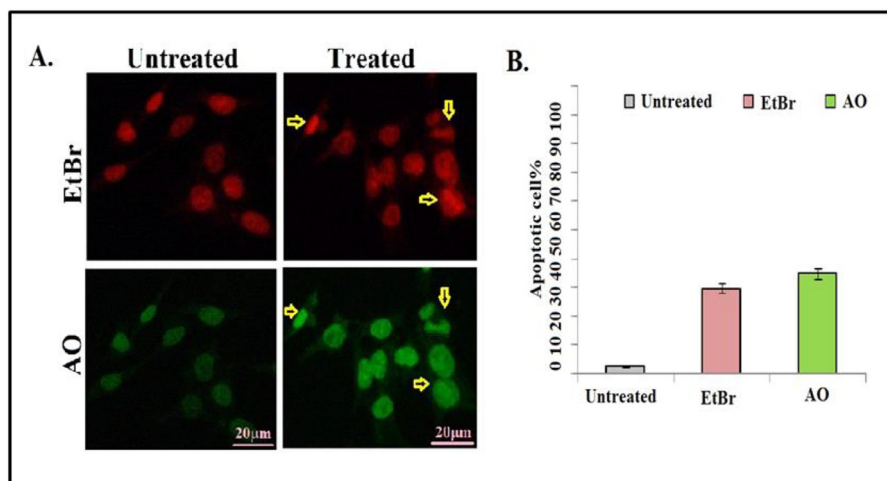


Fig. 7. The figure focuses on the treatment of OVCAR-3 cancer cells with the methanolic extract of *A. ornatooides* at a specific IC_{50} concentration, which is 38 $\mu\text{g/ml}$. Part A of the figure includes an image captured by microscope. This image shows OVCAR-3 cancer cells that have been stained with two dyes: Ethidium Bromide (EtBr) and Acridine orange (AO). These stains are often used to distinguish between live and apoptotic cells. The apoptotic cells have been marked in the image. It specifies the magnification level (200X) and the scale bar (20 μm), indicating the size represented in the image. Part B of the figure represents a graph, which shows the viability and apoptotic percentage of the OVCAR-3 cancer cells. This graph presents data quantifying the effects of the methanolic extract treatment at the IC_{50} concentration on OVCAR-3 cells. It shows the number of viable cells and cells that have undergone apoptosis (cell death) as a result of the treatment. The graph also includes error bars or a standard deviation to indicate the viability in the data.

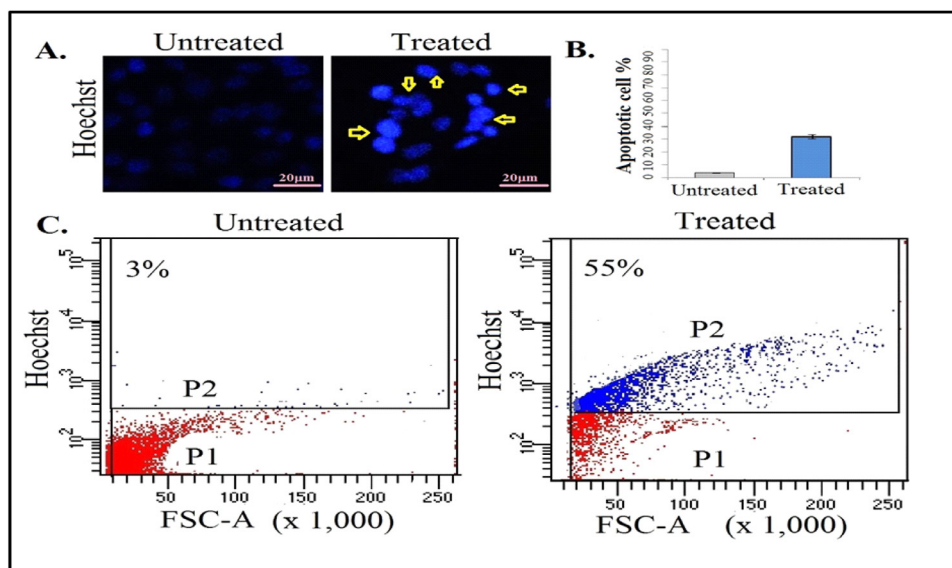


Fig. 8. Provides a comprehensive visual representation of the impact of methanolic extract on OVCAR-3 cancer cells at the IC_{50} concentration. Part A shows the morphology of the cells, highlighting apoptotic cells, part B quantifies the viability and apoptotic cell percentage, and part C provides additional evidence of apoptotic cell death through flow cytometry analysis. This data is essential for evaluating the potential anticancer properties of the lichen extract and its effects on OVCAR-3 cell.

exhibit significant reduction in cellular stress generated by both ROS and NO_2 (Fig. 10A & B), and reduced inflammation (Fig 11A & B).

The role of inflammation in cancer is a complex and well-studied area in cancer biology. Inflammation is a natural immune response by the body to fight infections, heal injuries, and repair damaged tissues. However, chronic inflammation, which persists over an extended period, can promote the development and progression of cancer in several ways. Inflammation can cause DNA damage and mutations in cells. When DNA damage is not repaired correctly, it can lead to the formation of cancerous cells. Chronic inflammation can create a microenvironment that is conducive to the growth of cancer cells (Lee et al., 2019; Li et al., 2021). It can stimulate the production of growth factors and cytokines that support tumor proliferation. Inflammation can interfere with the normal functioning of the immune system. It can inhibit the immune system's ability to recognize and destroy cancer cells, allowing them to evade detection.

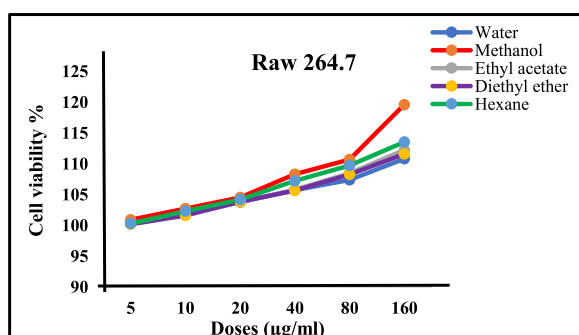


Fig. 9. Proliferation of Raw 264.7 macrophage cells with the increasing concentration of all the extracts. The study focuses on a specific type of immune cell line called Raw 264.7. Macrophages are immune cells that play a crucial role in the body's defence against pathogens and can be involved in various immune responses. The figure represents the methanolic extract of *A. ornatoides* influences the proliferation of Raw 264.7 macrophage cells, with the X-axis showing increasing concentrations of the extract and the Y-axis representing the level of cell proliferation. This data is important for assessing the potential immunomodulatory or stimulatory properties of the lichen extract on macrophage cells.

Inflammation can promote the formation of new blood vessels (angiogenesis) that supply nutrients and oxygen to tumor, enabling their growth and spread. Given the role of inflammation in cancer, there is significant interest in developing natural therapeutic approaches, such as the use of lichens, as immunomodulators and anticancer agents.

3.13. In-vitro toxicity analysis

Fig. 12.

3.14. In-vivo toxicity analysis

Fig. 14.

4. GC–MS

The chemical composition volatile compounds of *A. ornatoides* were determined by GC–MS (Fig. 13). In total, 21 volatile compounds have been identified (Table 5), which represents three major compounds, viz., methoxyylivetol (78.91 %), imidazole 2-t-butyl-1,4-dimethyl-5-phenyl (6.32 %) and benzoic acid 2,4-dihydroxy-3,6-dimethyl-methyl ester (4.77 %).

5. Discussion

Lichens are remarkable organisms that have thrived for centuries in some of the harshest environments on Earth. These unique symbiotic associations of fungi and photosynthetic organisms have long captured the attention of scientists and naturalists. Beyond their ecological significance, lichens have been recognized for their pharmacological potential, offering a rich source of bioactive compounds. Antioxidants are well-known for their capacity to combat oxidative stress, which is implicated in the development of various diseases, including cancer, immune system dysregulation, and inflammatory disorders. The assessment of *Anzia ornatoides* for its therapeutic potential presents an exciting intersection of traditional ecological knowledge and modern scientific research. This lichen's history of use in traditional medicine, coupled with its antioxidant richness, has

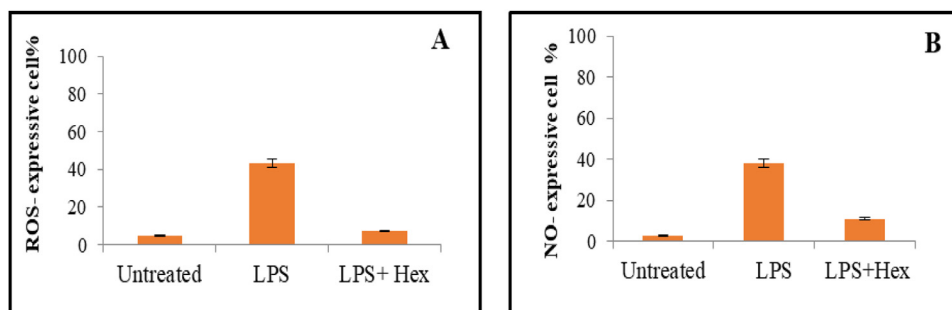


Fig. 10. The Raw 264.7 cells were treated with the methanol extract at the EC₅₀ concentration. EC₅₀ is expected to have half of its maximal effect. The Y-axis of the graph represents the percentage of expression of ROS and NO₂. ROS and NO₂ are molecules often associated with cellular stress, inflammation, and immune responses. This percentage indicates the level of these molecules being produced by the Raw 264.7 cells when treated with the extract at the EC₅₀ concentration. The X-axis typically represents the experimental conditions of treatments. In this case, it would show different groups or time points related to the treatment of Raw 264.7 cells with the extract at the EC₅₀ concentration. The graph shows data points or curves that show the percentage of ROS and NO₂ expression under different experimental conditions. It has been represented as different bars, lines, or data points on the graph.

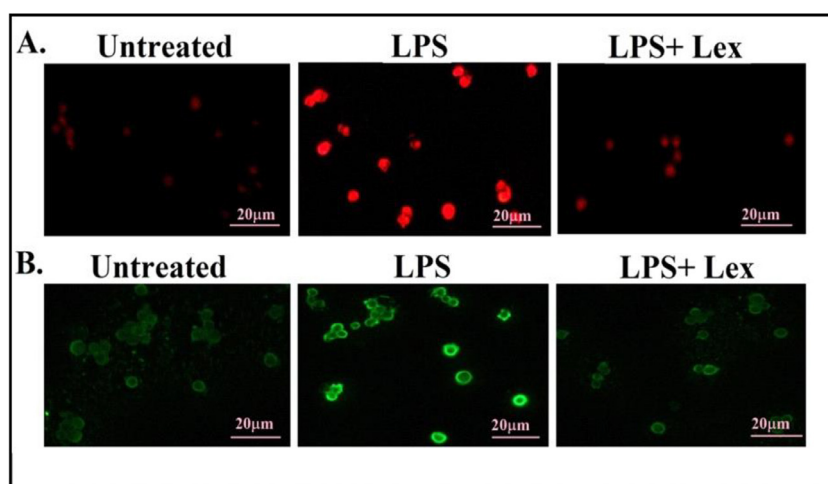


Fig. 11. The figure visually demonstrates the anti-inflammatory effects of the methanolic extract of *A. ornatooides* on macrophage cells that were previously induced to exhibit inflammation. Part A shows a reduction in ROS, and Part B shows a reduction in NO₂, both of which are indicators of reduced inflammation. These images provide direct evidence of the extract's potential anti-inflammatory properties, which can be crucial in understanding its therapeutic effects on inflammation-related conditions.

prompted rigorous investigation into its possible benefits for human health.

Lichen extracts exhibited a fairly strong antioxidant activity which is interrelated with phenol and flavonoid compounds, shows significantly a stronger radical scavenging effects owing to their capability to neutralize free radicals such as superoxide, singlet oxygen and hydroxyl radical. Different extraction solvent results varied due to their chemical compositions. The results of cytotoxicity assay displayed the selected lichen used in this study exerts cytotoxic and apoptotic activity on cell lines. The loss of viability of cell lines as proved by morphological changes were examined by confocal microscopy. The discovery of this work supports the extracts of *A. ornatooides* significantly an effective radical scavenger with anti-inflammatory and immunomodulatory effects represents the presence of many natural antioxidants or active bioactive compounds with desired therapeutic potential. Flow cytometric studies proposed the species induced apoptosis in cell lines and no cellular toxicity in-vitro cultured cells and tissue damage in-vivo experiment with mice was observed in liver and kidney with toxicity studies.

The findings of our study provide compelling evidence of the multifaceted health benefits of *Anzia ornatooides*, highlighting its potential as a valuable source of natural remedies. We have delved into the key aspects of our investigation. Our research supports the notion that

Anzia ornatooides exhibits significant anticancer potential agent. In vitro studies demonstrated that extracts of this lichen inhibited the proliferation of several cancer cell lines PC-3, OVCAR-3, MCF-7, HeLa, Hep-G2, and h-1299. This antiproliferative effect was particularly notable in all the cancer cells. Further in vivo studies using animal models revealed as nontoxic in lichen-treated groups. The mechanisms underlying these anticancer effects appear to involve the induction of apoptosis and the inhibition of which is a vital process in tumor development. *Anzia ornatooides* demonstrated promising immunomodulatory effects in our experiments. We observed an enhancement of immune responses. These findings are significant for the potential treatment of immune-related disorders. Our results also suggest a potent anti-inflammatory capacity of *Anzia ornatooides*. Inflammatory markers and mediators were notably reduced in models of acute and chronic inflammation following lichen treatment. These findings hold great promise for the development of anti-inflammatory agents. However, the biological properties of this lichen remain to be investigated and to the best of our knowledge, this is the first report of antioxidant, immunomodulatory, anti-inflammatory and anticancer activities of *A. ornatooides*. While there is promising preclinical research on the anticancer potential of lichens, it's essential to note that the transition from laboratory studies to effective clinical therapies is a complex process. Clinical trials are

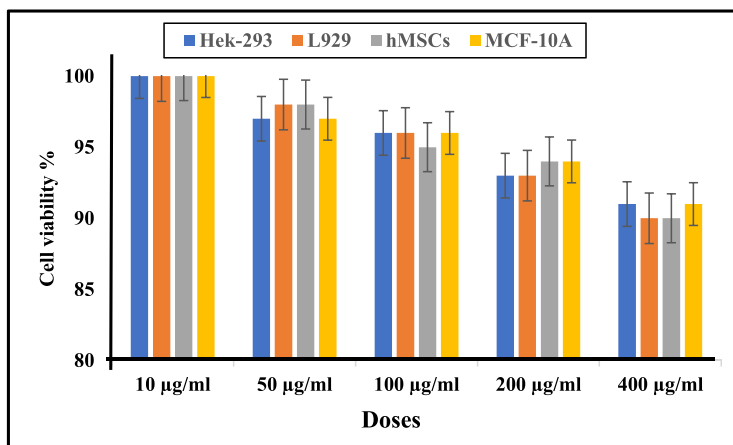


Fig. 12. The figure demonstrates the extract influences viability and apoptotic cell death of healthy cells across a range of concentrations. The X-axis of each graph represents concentration of the methanolic extract, ranging from 10 µg/ml to 400 µg/ml. This range represents different concentrations at which the extract was applied to the healthy cells. The Y-axis of the graphs represent different measures. Here, there are two measures mentioned viability and apoptotic cell death percentages. The graphs identify the concentration at which the extract has the most significant effect on either promoting cell death (apoptosis) or preserving cell viability. It shows the safety and potential therapeutic effects of the extract on healthy cells. It can help determine the extract’s cytotoxicity, which is its ability to cause cell death, as well as any potential benefits in terms of apoptosis induction, which might be desirable in certain medical contexts.

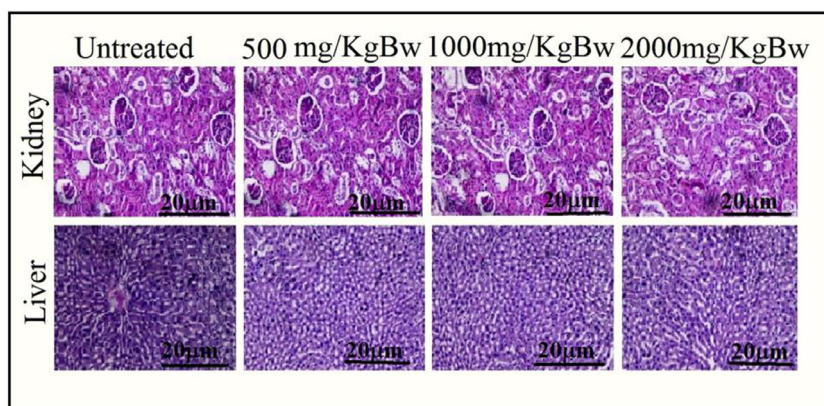


Fig. 13. The panels compare untreated animals (control group) to animals that have been treated with increasing concentrations of the methanolic extract. These concentrations may vary, and the experiment have used multiple doses to assess the extract’s impact on the tissues. Each panel includes a scale bar, which helps viewers understand the size represented in the images. In this case, the scale bar indicates that 20 µm in the images corresponds to a specific length in reality. Additionally, the images are captured at a magnification of 200X, which means they are viewed under a microscope 200 times larger than their actual size. The figure suggests that, at the tested concentrations, the extract did not cause significant visible damage or abnormalities in the structure and morphology of these tissues. Histological staining and microscopy to assess the condition of kidney and liver tissues in response to treatment with the methanolic extract. The observations indicate that the tissues maintain their normal appearance and structure, suggesting that the extract may be well-tolerated by these organs at the concentrations tested.

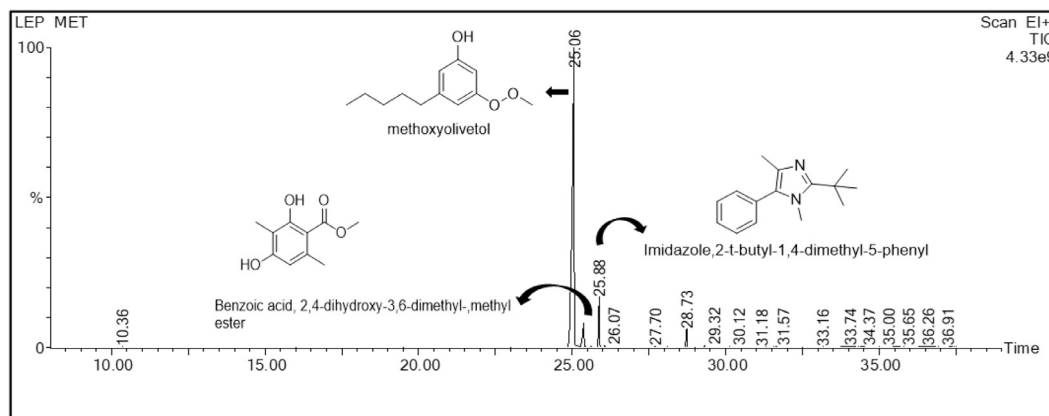


Fig 14. GC–MS chromatograph of the methanol extract of *A. ornatoides* volatile compounds with putative chemical structures of most abundant molecule.

Table 5
Compounds Detected and identified in the methanol extract by GC–MS.

Sl No.	Name of the compound	RT (min)	Peak area (%)	M.W.
1	Benzeneacetaldehyde	15.541	0.017	120
2	Phosphonic acid, (p-hydroxyphenyl)-	10.359	0.103	174
3	Hydroquinone	16.542	0.123	110
4	2(1 h)-pyridinone, 3-amino-	17.012	0.124	110
5	1-propanamine, 3-(2-methoxy-1-methylethoxy)-	18.032	0.057	147
6	.Alpha.-[2-piperidyl]-2-trifluoromethyl-6,8-dichloro-4-Quinolinemethanol	18.973	0.047	378
7	Methoxyolivetol	25.055	78.916	194
8	Benzoic acid, 2,4-dihydroxy-3,6-dimethyl-, methyl ester	25.37	4.77	196
9	Imidazole, 2-t-butyl-1,4-dimethyl-5-phenyl	25.881	6.324	228
10	1,3-benzenediol, 5-pentyl-	26.066	0.214	180
11	Pyrazole-4-carboxaldehyde, 3-(4-chlorophenyl)-	27.701	0.19	206
12	Pyrazole, 3-(p-chlorophenyl)-5-methyl-	28.096	0.054	192
13	O-anisic acid, 4-hydroxy-6-pentyl-, methyl ester, ester with 2-hydroxy	28.732	2.393	514
14	Octadecanoic acid	29.317	0.179	284
15	2,6,10-dodecatrien-5-one, 1-(2,5-dihydroxy-3-methylphenyl)-3,7,11-trimethyl	30.117	0.057	422
16	Z,Z,Z-8,9-epoxyeicosa-5,11,14-trienoic acid, methyl ester	31.183	0.036	334
17	Cyclohexanol, 5-methyl-2-(1-methylethyl)-, [1s-(1.alpha.,2.beta.,5.beta.)]	31.318	0.07	156
18	1-methylene-2b-hydroxymethyl-3,3-dimethyl-4b-(3-methylbut-2-enyl)-cy	31.638	0.125	222
19	Alpha.-linolenic acid, tms derivative	33.864	0.506	350
20	2(1 h)-benzocyclooctenone, decahydro-10a-methyl-, trans-	36.42	0.299	194
21	2-oxo-2,3-dihydro-1h-imidazole-4-carbonitrile	36.675	0.206	109

Table 6
Kruskal-Wallis Anova of TPC and TFC and Phosphomolybdenum assay between the extracts.

Assays	²	df	P-value	Significance
TPC	13.57	4	0.009	**
TFC	13.66	4	0.008	**
Phosphomolybdenum assay	13.77	4	0.008	**
FRAP	14	4	0.007	**

The populations are significantly different (**: $P < 0.01$).

Table 7a
Kruskal-Wallis Anova of DPPH between the extracts in each concentration.

Concentration	²	df	P-value	Significance
10	11.49	4	0.02	*
20	12.92	4	0.01	**
30	13.5	4	0.009	**
40	13.54	4	0.008	**
50	12.92	4	0.01	**

The populations are significantly different (*: $P < 0.05$, **: $P < 0.01$).

Table 7b
Kruskal-Wallis Anova of DPPH between the concentration in each extract.

Extracts	²	df	P-value	Significance
Hexane	10.12	4	0.04	*
Diethyl ether	13.26	4	0.01	**
Ethyl acetate	13.50	4	0.009	**
Methanol	13.55	4	0.008	**
Water	13.55	4	0.008	**

The values are significantly different (*: $P < 0.05$, **: $P < 0.01$).

Table 8a
Kruskal-Wallis Anova of ABTS between the extracts in each concentration.

Concentration	²	df	P-value	Significance
10	12.26	4	0.01	**
20	13.55	4	0.009	**
30	13.52	4	0.008	**
40	13.50	4	0.009	**
50	13.55	4	0.008	**

The values are significantly different (**: $P < 0.01$).

Table 8b
Kruskal-Wallis Anova of ABTS between the concentration in each extract.

Extracts	²	df	P-value	Significance
Hexane	13.52	4	0.009	**
Diethyl ether	13.23	4	0.01	**
Ethyl acetate	13.55	4	0.008	**
Methanol	13.52	4	0.008	**
Water	13.28	4	0.009	**

The values are significantly different (**: $P < 0.01$).

Table 9a
Kruskal-Wallis Anova of lipid peroxidation between the extracts in each concentration.

Concentration	²	df	P-value	Significance
10	13.16	4	0.01	**
20	12.95	4	0.01	**
30	11.79	4	0.02	*
40	13.23	4	0.01	*
50	13.15	4	0.01	**

The values are significantly different (*: $P < 0.05$, **: $P < 0.01$).

needed to assess the safety and efficacy of lichen-derived compounds in humans. Additionally, the specific lichen species, extraction methods, and compounds involved may vary, making it important to identify and study the most promising candidates.

Table 9b

Kruskal-Wallis Anova of lipid peroxidation between the concentration in each extract .

Extracts	²	df	P-value	Significance
Hexane	13.60	4	0.008	**
Diethyl ether	13.43	4	0.009	**
Ethyl acetate	13.60	4	0.008	**
Methanol	13.55	4	0.008	**
Water	13.77	4	0.008	**

The values are significantly different (**: $P < 0.01$).

6. Conclusion

In conclusion, the comprehensive investigations conducted in this study provide compelling evidence for the remarkable potential of the lichen's extract under examination as a promising candidate for anticancer, anti-inflammatory, and immunomodulatory therapy. Through a series of meticulously designed experiments, including cell proliferation assay, apoptosis assay, anti-ROS evaluation, and toxicological assessment, we have unveiled the multifaceted properties of this extract. Our results consistently demonstrated the extract's ability to inhibit cancer cell proliferation and induce apoptosis, highlighting its potent anticancer properties. Additionally, its anti-inflammatory effects were evident through the reduction of pro-inflammatory markers and the mitigation of oxidative stress, further supporting its potential as an anti-inflammatory agent. Furthermore, the immunomodulatory activity of the *A. ornatooides* extract was underscored by its capacity to modulate immune responses, potentially opening new avenues for treating immune-related disorders. Importantly, the toxicological evaluation revealed a favourable safety profile, which is crucial for the development of therapeutic agents. In light of these findings, our study underscores the significance of exploring *A. ornatooides* extracts as valuable resources in the development of novel therapies. While further research is necessary to elucidate the underlying mechanisms and optimize dosages for clinical applications, the promising outcomes of this investigation warrant continued exploration of this lichen and extract's potential in the fields of cancer treatment, anti-inflammatory therapy, and immunomodulation. This research serves as a foundation for future studies aimed at harnessing the full therapeutic potential of this natural compound for the benefit of human health.

Declaration of Competing Interest

The authors have no conflict of interest

Acknowledgement

This study was supported by the Department of Botany, Bodoland University, Kokrajhar, Assam. We would like to acknowledge Centre for Excellence in Natural Product & Therapeutics, Department of Biotechnology and Bioinformatics Sambalpur University, Odisha and Institute of Life sciences Bhubaneswar, Odisha. Siksha 'O' Anusandhan Deemed to be University, Odisha for their valuable suggestion and support.

References

Adenubi, O.T., Famuyide, I.M., McGaw, L.J., Eloff, J.N., 2022. Lichens: an update on their ethnopharmacological uses and potential as sources of drug leads. *J. Ethnopharmacol.* 298, 115657. <https://doi.org/10.1016/j.jep.2022.115657>.

Alpay, M., Backman, L.R.F., Cheng, X.D., Dukel, M., Kim, W.J., Ai, L.B., Brown, K.D., 2015. Oxidative stress shapes breast cancer phenotype through chronic activation of ATM-dependent signaling. *Breast Cancer Res. Treat.* 151, 75–87. <https://doi.org/10.1007/s10549-015-3368-5>.

Ananthi, R., Tinabaye, A., Selvaraj, G., 2015. Antioxidant study of Usnic acid and its derivative Usnic acid diacetate. *Int. J. Res. Eng. Technol.* 4, 356–366. <https://doi.org/10.15623/ijret.2015.0402047>.

Awasthi, D.D., 2007. *A Compendium of the Macrolichens from India, Nepal, Sri Lanka, 1st ed.* Bishen Singh Mahendra Pal Singh, Dehra Dun, India.

Behera, S., Mohapatra, S., Meher, R.K., Das, P.K., Babu, S.K., Naik, M., Monalisa, Naik, S.K., Naik, P.K., 2023. Assessment of Chemical Composition and Therapeutic Activities of *Clausena excavata* Burm.: an important medicinal plant of eastern Ghats of India. *J. Essent. Oil Bear. Plants* 26, 502–521. <https://doi.org/10.1080/0972060X.2023.2216721>.

Borkakoty, M., Kakoty, B.B., Saikia, L., 2013. Influence of total phenolic and total flavonoid content on the DPPH radical scavenging activity of *Eclipta alba* (L.) Hassk. *Int. J. Pharm. Pharm. Sci.* 5, 324–327.

Calcott, M.J., Ackerley, D.F., Knight, A., Keyzers, R.A., Owen, J.C., 2018. Secondary metabolism in the lichen symbiosis. *Chem. Soc. Rev.* 47, 1730–1760. <https://doi.org/10.1039/C7CS00431A>.

Chohra, D., Ferchichi, L., Cakmak, Y.S., Zengin, G., Alsheikh, S.M., 2020. Phenolic profiles, antioxidant activities and enzyme inhibitory effects of an Algerian medicinal plant (*Clematis cirrhosa* L.). *S. Afr. J. Bot.* 132, 164–170. <https://doi.org/10.1016/j.sajb.2020.04.026>.

Dar, T.U.H., Dar, S.A., Islam, S.U., Mangral, Z.A., Dar, R., Singh, B.P., Verma, P., Haque, S., 2022. Lichens as a repository of bioactive compounds: an open window for green therapy against diverse cancers. *Semin. Cancer Biol.* 86, 1120–1137.

Dobros, N., Zawada, K., Paradowska, K., 2022. Phytochemical Profile and Antioxidant Activity of *Lavandula angustifolia* and *Lavandula x intermedia* Cultivars Extracted with Different Methods. *Antioxidants* 11, 711. <https://doi.org/10.3390/antiox11040711>.

Dorman, H.J., Bachmayer, O., Kosar, M., Hiltunen, R., 2004. Antioxidant properties of aqueous extracts from selected Lamiaceae species grown in Turkey. *J. Agric. Food Chem.* 52, 762–770. <https://doi.org/10.1021/jf034908v>.

El-Garawani, I.M., Elkhateeb, W.A., Zaghlol, G.M., Almeer, R.S., Ahmed, E.F., Rateb, M.E., Abdel Moneim, A.E., 2019. *Candelariella vitellina* extract triggers in-vitro and in-vivo cell death through induction of apoptosis: a novel anticancer agent. *Food Chem. Toxicol.* 127, 110–119. <https://doi.org/10.1016/j.fct.2019.03.003>.

Forcados, G.E., Chinyere, C.N., Shu, M.L., 2016. *Acalypha wilkesiana*: therapeutic and toxic potential. *J. Med. Surgical Pathol.* 1, 122. <https://doi.org/10.4172/2472-4971.1000122>.

Gadow, A., Joubert, E., Hansmann, C.F., 1997. Comparison of the antioxidant activity of aspalathin with that of other plant phenols of Rooibos Tea (*Aspalathus linearis*), α -tocopherol, BHT and BHA. *J. Agric. Food Chem.* 45, 632–638. <https://doi.org/10.1021/jf960281n>.

Gandhi, A.D., Umamaheshc, K., Sathiyaraj, S., Suriyakalaa, G., Velmurugand, R., Farraj, D.A.A., Gawwadf, M.R.A., Murugang, K., Babujanarthanama, R., Saranya, R., 2022. Isolation of bioactive compounds from lichen *Parmelia sulcata* and evaluation of antimicrobial property. *J. Infect Public Health* 15, 491–497. <https://doi.org/10.1016/j.jiph.2021.10.014>.

Hajam, Y.A., Rani, R., Ganie, S.Y., Sheikh, T.A., Javaid, D., Qadri, S.S., Pramodh, S., Alsulimani, A., Alkhanani, M.F., Harakeh, S., Hussain, A., Haque, S., Reshi, M.S., 2022. Oxidative stress in human pathology and aging: molecular mechanisms and perspectives. *Cells* 11, 552. <https://doi.org/10.3390/cells11030552>.

Hsu, C.K., Chiang, B.H., Chen, Y.S., Yang, J.H., Liu, C.L., 2008. Improving the antioxidant activity of buck wheat (*Fagopyrum tataricum* Gaertn) sprout with trace element water. *Food Chem.* 108, 633–641. <https://doi.org/10.1016/j.foodchem.2007.11.028>.

Kim, G.H., Kim, J.E., Rhie, S.J., Yoon, S., 2015. The role of Oxidative Stress in neurodegenerative diseases. *Exp. Neurobiol.* 24, 325–340. <https://doi.org/10.5607/en2015.24.4.325>.

Lee, C., Do, H.T.T., Her, J., Kim, Y., Seo, D., Rhee, I., 2019. Inflammasome as a promising therapeutic target for cancer. *Life Sci.* 231, 116593. <https://doi.org/10.1016/j.lfs.2019.116593>.

Li, Y., Huang, H., Liu, B., Zhang, Y., Pan, X., Yu, X.Y., Song, Y.H., 2021. Inflammasomes as therapeutic targets in human diseases. *Signal Transduct. Targeted Therapy* 6, 247. <https://doi.org/10.1038/s41392-021-00650-z>.

Lompo, M., Traore acute, R., Oueacutedraogo, N., Kinieacute lix, F., Tibirieacute, A., Duez, P., Guissou, I.P., 2016. In-vitro antioxidant activity and phenolic contents of different fractions of ethanolic extract from *Khaya senegalensis* A. Juss. (Meliaceae) stem barks. *Afr. J. Pharm. Pharmacol.* 10, 501–507. <https://doi.org/10.5897/AJPP2016.4564>.

Mbaoji, F.N., Nweze, J.A., 2020. Antioxidant and hepatoprotective potentials of active fractions of *Lamnea barteri* Oliv. (Anarcadiaceae) in rats. *Heliyon* 6, e04099. <https://doi.org/10.1016/j.heliyon.2020.e04099>.

Meda, A., Lamien, C.E., Romito, M., Millogo, J., Nacoulma, O.G., 2005. Determination of the total phenolic, flavonoid and proline contents in Burkina Fasan honey, as well as their radical scavenging activity. *Food Chem.* 91, 571–577. <https://doi.org/10.1016/j.foodchem.2004.10.006>.

Meher, R.K., Naik, M.R., Bastia, B., Naik, P.K., 2018. Comparative evaluation of anti-angiogenic effects of noscapine derivatives. *Bioinformation* 14, 236–240. <https://doi.org/10.6026/97320630014236>.

Meher, R.K., Pragyaandipta, P., Pedapati, R.K., Nagireddy, P.K., Kantevari, S., Nayek, A.K., Naik, P.K., 2021a. Rational design of novel N-alkyl amine analogues of noscapine, their chemical synthesis and cellular activity as potent anticancer agents. *Chem. Biol. Drug Des.* 98, 445–465. <https://doi.org/10.1111/cbdd.13901>.

Meher, R.K., Pragyaandipta, P., Reddy, P.K., Pedapati, R., Kantevari, S., Naik, P.K., 2021b. Development of 1, 3-diylnyl derivatives of noscapine as potent tubulin binding anticancer agents for the management of breast cancer. *J. Biomol. Struct. Dyn.* 40, 13136–13153. <https://doi.org/10.1080/07391102.2021.1982008>.

Mir, S.A., Padhiary, A., Pati, A., Tete, S.S., Meher, R.K., Baitharu, I., Muhammad, A., Nayak, B., 2023. Potential phytochemicals as microtubule-disrupting agents in cancer prevention. *Recent Frontiers of Phytochemicals* pp. 225–246.

- Neilson, A.P., Goodrich, K.M., Ferruzzi, M.G., 2017. Bioavailability and metabolism of bioactive compounds from foods, In Nutrition in the Prevention and Treatment of Disease. 4th ed. Elsevier Inc., San Diego, CA, USA. <https://doi.org/10.1016/B978-0-12-802928-2.00015-1>.
- Nguyen-Trinh, Q.N., Trinh, K.X.T., Trinh, N.T., Vo, V.T., Li, N., Nagasaki, Y., Vong, L.B., 2022. A silica-based antioxidant nanoparticle for oral delivery of Camptothecin which reduces intestinal side effects while improving drug efficacy for colon cancer treatment. *Acta Biomater.* 143, 459–470. <https://doi.org/10.1016/j.actbio.2022.02.036>.
- Nur, S., Mubarak, F., Jannah, C., Winarni, D.A., Rahman, D.A., Hamdayani, L.A., Sami, F.J., 2019. Total phenolic and flavonoid compounds, antioxidant and toxicity profile of extract and fractions of pakuatai tuber (*Angiopteris ferox* Copel). *Food Res.* 3, 734–740. [https://doi.org/10.26656/fr.2017.3\(6\).135](https://doi.org/10.26656/fr.2017.3(6).135).
- Oyaizu, M., 1986. Studies on products of browning reaction prepared from glucose-amine. *Jpn. J. Nutr.* 44, 307–315. <https://doi.org/10.5264/eiyogakuzashi.44.307>.
- Pham, N.K.T., Nguyen, H.T., Dao, T.B.N., Vu-Huynh, K.L., Nguyen, T.Q.T., Huynh, B.L.C., Le, T.D., Nguyen, N.H., Nguyen, N.H., Duong, T.H., 2021. Two New Phenolic Compounds from the Lichen *Parmotrema cristiferum* Growing in Vietnam. *Nat. Prod. Res.* 36, 3865–3871. <https://doi.org/10.1080/14786419.2021.1892672>.
- Pisoschi, A.M., Pop, A., 2015. The role of antioxidants in the chemistry of oxidative stress: a review. *Eur. J. Med. Chem.* 97, 55–74. <https://doi.org/10.1016/j.ejmech.2015.04.040>.
- Pradhan, S., Upreti, D.K., Meher, R.K., Satapathy, K.B., 2022. Antimicrobial, anticancer, and antioxidant potential of two dominant macro-lichen *Dirinaria aegialita* and *Parmotrema praesorediosum* collected from Similipal Biosphere Reserve of Odisha, India. *J. Appl. Biol. Biotechnol.* 10, 34–43. <https://doi.org/10.7324/JABB.2022.100604>.
- Prieto, P., Pineda, M., Aguilar, M., 1999. Spectrophotometric quantitation of antioxidant capacity through the formation of a phosphomolybdenum complex: specific application to the determination of vitamin E. *Anal. Biochem.* 26, 337–341. <https://doi.org/10.1006/abio.1999.4019>.
- Re, R., Pellegrini, N., Proteggente, A., Pannala, A., Yang, M., RiceEvans, C., 1999. Antioxidant activity applying an improved ABTS radical cation decolorization assay. *Free Radical Biol. Med.* 26, 1231–1237. [https://doi.org/10.1016/S0891-5849\(98\)00315-3](https://doi.org/10.1016/S0891-5849(98)00315-3).
- Saed, G.M., Diamond, M.P., Fletcher, N.M., 2017. Updates of the role of oxidative stress in the pathogenesis of ovarian cancer. *Gynecol. Oncol.* 145, 595–602. <https://doi.org/10.1016/j.ygyno.2017.02.033>.
- Saluja, T.S., Kumar, V., Agrawal, M., Tripathi, A., Meher, R.K., Srivastava, K., Gupta, A., Singh, A., Chaturvedi, A., Singh, S., 2020. Mitochondrial stress-mediated targeting of quiescent cancer stem cells in oral squamous cell carcinoma. *Cancer Manag. Res.* 12, 4519–4530. <https://doi.org/10.2147/CMAR.S252292>.
- Saroyo, H., Nur, I.A.A., 2020. Antioxidant activity using DPPH and FRAP Method and their correlation with the levels of Phenolic and Flavonoid Compounds from Nemba Plants (*Azadirachta indica* A. Juss). *J. Nutraceuticals Herb. Med.* 3, 10–20. <https://doi.org/10.23917/jnhm.v3i2.15658>.
- Singh, K.P., Sinha, G.P., 2010. Indian Lichens: an Annotated Checklist. Bishen Singh Mahendra Pal Singh, Dehradun, India.
- Slinkard, K., Singleton, V.L., 1997. Total phenolic analyses: automation and comparison with manual method. *Am. J. Enol. Vitic.* 28, 49–55.
- Stocker-Wörgötter, E., 2008. Metabolic diversity of lichen-forming ascomycetous fungi: culturing, polyketide and shikimate metabolic production and PKS genes. *Nat. Prod. Rep.* 25, 188–200. <https://doi.org/10.1039/B606983P>.
- Vyas, S., Kachhwaha, S., Kothari, S.L., 2015. Comparative analysis of Phenolic contents and total antioxidant capacity of *Moringa oleifera* Lam. *Pharmacognosy J.* 7, 44–51. <https://doi.org/10.5530/pj.2015.7.5>.
- Yurdacan, B., Egel, U., GuneyEskiler, G., Eryilmaz, I.E., Cecener, G., Tunca, B., 2019. The role of usnic acid-induced apoptosis and autophagy in hepatocellular carcinoma. *Hum. Exp. Toxicol.* 38, 201–215. <https://doi.org/10.1177/0960327118792052>.
- Zawawi, N., Chong, P.J., Mohd Tom, N.N., Anuar, N.S.S., Mohammad, S.M., Ismail, N., Jusoh, A.Z., 2021. Establishing relationship between vitamins, total phenolic and total flavonoid content and antioxidant activities in various honey types. *Molecules* 26, 4399. <https://doi.org/10.3390/molecules26154399>.
- Zhao, H., Wu, L., Yan, G., Chen, Y., Zhou, M., Wu, Y., Li, Y., 2021a. Inflammation and tumor progression: signaling pathways and targeted intervention. *Signal Transduction Targeted Therapy* 6, 1–46. <https://doi.org/10.1016/j.actbio.2022.02.036>.
- Zhao, Y., Wang, M., Xu, B., 2021b. A comprehensive review on secondary metabolites and health-promoting effects of edible lichen. *J. Funct. Foods* 80, 104283. <https://doi.org/10.1016/j.jff.2020.104283>.